APPLICATIONS OF STRAIN CYCLING CONSIDERATIONS

TO SUPERHEAT FUEL DESIGN

by

G. F. Rieger

ATOMIC POWER EQUIPMENT DEPARTMENT

GENERAL ⓖⓔ ELECTRIC

SAN JOSE, CALIFORNIA

TABLE OF CONTENTS

LIST OF ILLUSTRATIONS

APPROVED:

S. Naymark, Manager
Fuels and Materials Development

L. Fiock
Project Engineer

ATOMIC POWER EQUIPMENT DEPARTMENT
GENERAL ELECTRIC
SAN JOSE, CALIFORNIA

1   SUMMARY

A potential performance limitation of superheat fuel is the susceptibility of the fuel cladding to low cycle fatigue failure. Two simplified analytical methods are presented to estimate the cyclic lifetime of circular superheat fuel cladding.

One failure relation, based on a displacement method, is of the form

$$N_f = 0.33 \left[\frac{C}{\Delta \epsilon_p} \right]^n \tag{1}$$

where

N_f = Cycles to failure

$\Delta \epsilon_p$ = Plastic strain range of the power cycle

C, n = Material property constants

The other failure relation, based on a stress method, is of the form

$$N_f = \frac{1}{12} \left[\frac{E C}{S - Se} \right]^2 \tag{2}$$

where

N_f = Cycles to failure

S = Elastic stress amplitude of the power cycle

E, C, Se = Material property constants

These relations were compared with data from the literature, and with data involving radiation damage obtained by Reynolds. [6] A recommended design procedure involving the relations is presented. The technique was applied to the SADE 4B experiment with moderate success.

These cycling relations involve only mechanical damage imposed by cycling, with a modification for additional damage caused by radiation; they do not include any other potential performance limiting mechanisms, such as stress corrosion, which are normally factored into the over-all fuel design.

This work was done under Task C (Materials Development) of the Nuclear Superheat Project, AEC Contract AT(04-3)189 - Project Agreement 13.

2. INTRODUCTION

One of the performance limitations of fuel cladding for superheat nuclear reactor service may be that which is associated with low cycle fatigue. The normal and transient operation of the reactor induce alternating loads on the fuel cladding, such as those by the expansion interaction of fuel and cladding, local discontinuities, coolant pressure, and temperature distributions. The effects of these loads are aggravated by the higher temperatures associated with superheat service, and can cause the cladding to undergo permanent deformations. When the permanent deformations alternate during operation, plastic strain cycling is caused, which can lead to low cycle fatigue, and hence, early failure of the fuel cladding.

Contributions to the literature by Coffin [1, 4], Manson [2], Swindeman and Douglas [3], and Langer [5], present various relations between the plastic strain range and cycles to failure. In general, these can be represented by the relation $N_f \Delta \epsilon_p^n = C$, where N_f is the cycles to failure, $\Delta \epsilon_p$ is the plastic strain range, and n and C are material constants. Recently, Reynolds [6] investigated the effect of neutron irradiation on the cyclic lifetime and has found that the lifetime is reduced when the material is subjected to fast neutron irradiation. It is the purpose of this, and several subsequent reports, to apply plastic cycling considerations to superheat fuel designs of circular geometries in order to reduce potential performance limitations. In turn, this should provide greater assurance that the integrity of the fuel cladding will be preserved, thereby extending the useful lifetime of the fuel.

Since strain cycling considerations are the primary interest of this report, other techniques of superheat fuel design will not be presented. These would include the standard elastic stress analyses, and effects of the coolant environment, such as stress corrosion.

It will be emphasized that the performance prediction based on the low cycle fatigue evaluation is not to be inferred as the only performance limitation; low cycle fatigue is evaluated on the structural, or mechanical, behavior of the cladding material only. It does not include other potential performance limitations such as those associated with stress corrosion. These other limitations may be considerably more severe than the fatigue limitation; however, the fatigue limitation should be evaluated, and factored into the cladding design considerations.

This report includes first, a presentation of the uniform strain cycle, and then perturbations to the uniform cycle caused by slight changes of the cladding radius of curvature, and by creep and relaxation effects. (Detailed development of severe localized effects, such as wrinkle formation and fuel discontinuities, are deferred to the next report.) Two methods of describing the fatigue parameters are presented; one is based on relative fuel and cladding displacements, and the other is based on an elastic stress amplitude. This is followed by a summary of some cyclic data from the literature, including the radiation effects presented by Reynolds. [6] These data can be used with the developed cycling parameters to predict the expected mechanical cyclic lifetime of the superheat fuel cladding.

3. UNIFORM STRAIN CYCLING - DISPLACEMENT METHOD

During operation, the reactor power is changed to accommodate the load demands placed upon it. The power changes, or power cycles, produce changes in the amount of expansion of the fuel and cladding. During operation at higher powers the fuel expands against the clad, and the inter- action may produce plastic strains. During operation at the lower power levels, the fuel con- tracts relative to the clad, and then the external coolant pressure acts to compress the cladding inward toward the fuel.

This action is typical for the cladding thicknesses of interest. In general, the wall thickness is small enough so that the cladding is elastically unstable, and requires support from the fuel to prevent collapse caused by the coolant pressure. When the cladding thicknesses are sufficient to withstand the coolant pressure without elastic collapse, the cladding is called free standing. When the as-built gap between fuel and clad is sufficiently small, or where operation at higher temperatures allows significant creep deformation to occur, nominally free-standing cladding may also be subject to plastic cycling.

In this section, uniform cycling means that throughout the complete cycle, the cross section of the cladding remains circular. It is expected that typical cladding behavior during operation will approximate the uniform cycling conditions for the major portions of the fuel lifetime. In addi- tion, the calculation results are relatively simple to obtain, which is advantageous for design purposes.

Two methods will be presented in Sections 3 and 4, both based on an infinite cylinder condition; the first is a displacement method determined from relative expansions, and the second is a fictitious stress method recently described by Tavernelli and Coffin. [4] Both consider a single description of the cycle, thus neglecting strain hardening, strain softening, and the Bauschinger effects.

For the displacement method in Section 3, a simplified creep effect is presented which may be added to the uniform cycle. This is utilized when the reactor design conditions include long time operation at high power between cycles.

3.1 Displacement Method

The displacement method of evaluating the uniform strains involves the relative movements of the fuel and cladding during the power cycle. This requires knowledge of the material properties, temperatures and thermal gradients, as well as the geometries of the fuel and cladding.

The cycle may be illustrated in terms of the stress strain diagram of the cladding material. As shown below, point o represents the first contact between the expanding fuel and cladding, where the fuel expansion has overcome not only the thermal expansion of the clad, but also whatever

gap that existed from fabrication. Point A' indicates the initial inelastic deformation of the clad. The deformation continues to A where the maximum strain occurs. When the power is reduced, and the fuel contracts, the coolant pressure compresses the cladding elastically, through point B. For cladding thicknesses of interest, if the initial strain is large enough, the compressive elastic limit will be exceeded, the clad displaces to the value indicated by C, and the stress state will be that corresponding to σ_C. (Release of the coolant pressure would allow the clad to expand to the equilibrium condition at point D.) If the power is increased from that corresponding to C to that of A, the deformation pattern is given by CDA. Subsequent cycling operation follows the path DABCD. As suggested by Coffin, the total strain range $\Delta\epsilon_T$ is given by $\epsilon_A - \epsilon_C$, and the plastic strain range $\Delta\epsilon_p$ by $\epsilon_B - \epsilon_D$.

The illustrated cycle considers only membrane-type expansions and contractions where the stress across the clad wall is essentially uniform. With the displacement method, the relative expansions or displacements, and the cladding stress-strain curve, completely define the state of uniform circumferential stress in the cladding. It should be restated that this includes the assumptions of an infinite length cylinder and significant plastic strains.
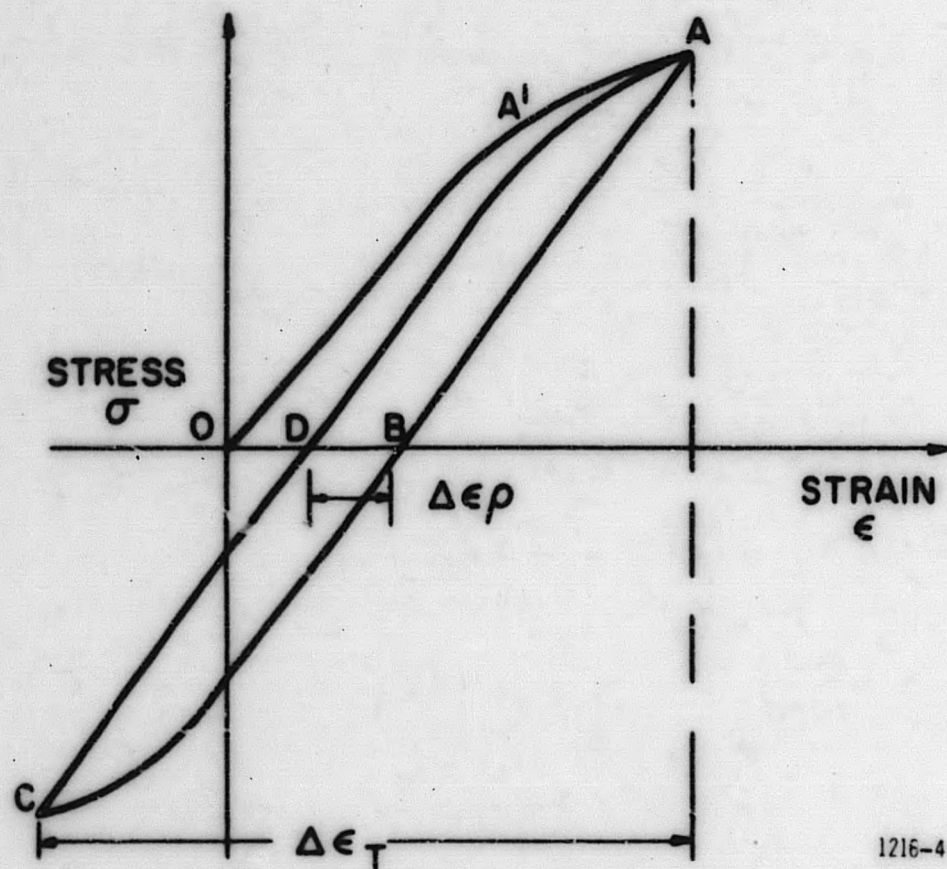
1216-4

Figure 3.1   Stress Strain Diagram of Cladding Material

3.2 Uniform Displacement Relations at Rated Power

The displacements may be determined from free expansion calculations. Neglecting fission gas pressures, the free diametral expansion of the cladding is that corresponding to the power level and temperature at A (P_A and T_A respectively) and is simply

$$\delta_{cl_A} = D \epsilon_{\theta cl_A} \tag{3}$$

where

δ_{cl_A} = Free diametral expansion of the clad to T_A

D = Mean diameter of the clad as fabricated

$\epsilon_{\theta cl_A}$ = Free circumferential thermal strain of the clad

and the latter term may be evaluated by

$$\epsilon_{\theta cl_A} = \Delta(\alpha_{cl}T) = \bar{\alpha}_{cl} (T_A - T_R) \tag{4}$$

where

$\bar{\alpha}_{cl}$ = Average coefficient of clad thermal expansion

T_R = Room temperature

The free expansion of the fuel may be treated in a similar manner. Thus

$$\delta_{f_A} = D \, \tilde{\epsilon}_{\theta f_A} \tag{5}$$

and the averaged thermal strain of the fuel is

$$\tilde{\epsilon}_{\theta f_A} = \bar{\alpha}_f (\bar{T}_{f_A} - T_R) \tag{6}$$

where

$\bar{\alpha}_f$ = Average coefficient of fuel thermal expansion. (For example, see reference 7.)

$\bar{T}_{f_A}$ = Volumetric average temperature of the fuel. (For example, see reference 8.)

As used here, $\tilde{\epsilon}_{\theta f_A}$ is a representative strain to establish the diametral expansion of the fuel,

and is not to be construed as the circumferential strain at the fuel surface. In practice, the fuel surface strains are sufficiently large to cause the cylindrical fuel to fracture. Thus, even though the fuel cylinder is made discontinuous and incapable of supporting symmetrical distributions of stress, for purposes of this work, the fuel is considered to be dimensionally stable, and expands and contracts radially as a single body.

The net interference between the clad and fuel may then be written as

$$\tilde{\delta}_{int_A} = \delta_{f_A} - \delta_{cl_A} - \delta_{gap_R} \qquad \text{(See also equation 13)} \qquad (7)$$

where

$$\delta_{gap_R} = \text{Diametral gap between clad and fuel as fabricated.}$$

and a required condition is that $\tilde{\delta}_{int_A} > 0$, the first time P_A is reached.

Then the uniform circumferential strain produced in the cladding at condition A may be written as

$$\epsilon_{cl-u_A} = \frac{\tilde{\delta}_{int_A}}{\bar{D}} \qquad \text{(See also equation 12)} \qquad (8)$$

For this simplified expression, the restraining action of the coolant pressure and the cladding hoop stress have been neglected. The coolant pressure may always be considered as a differential pressure reduction to the fuel hydrostatic type expansion pressure. However, for thicker clads, the restraining effect of the clad should be included. The clad restraint effect has been examined previously as part of the superheat program, and data obtained from tests conducted at the General Electric Test Reactor are presented by Lyons, et al. [9] However, since a power reactor can be expected to operate at the rated power conditions for a period of time, the relatively high stress σ_A, and temperature T_A, will cause creep and relaxation effects in the cladding. These will tend to relieve both the deformation and stress levels in the clad, and so modify the simple cycle DABCD considered here. These effects are discussed more fully in later sections. For the present, the free expansion relations are conservative in that shorter lifetimes are predicted.

Thermal Strain at Rated Power

Depending on the heat flux and clad thickness, a thermal strain is induced in the clad by the radial thermal gradient, $\partial T/\partial r$. This self-equilibriating effect may be superposed on the uniform strain given by (8). For the clad thicknesses of interest, the thermal gradient may be considered linear. Then the gradient strain may be written as

$$\epsilon_{\theta \Delta T_A} = \pm \frac{\alpha_{cl_A}}{2} \Delta T_{cl_A} \qquad \begin{array}{l} \text{+ or tensile on surface adjacent to coolant (9)} \\ \text{- or compressive on surface adjacent to fuel} \end{array}$$

where

α_{cl_A} = Thermal expansion coefficient of clad at T_A.

ΔT_{cl_A} = Temperature difference across clad wall at rated power P_A.

The temperature difference may be written in terms of the heat flux as

$$\Delta T_{cl_A} = \frac{q}{A} \frac{h}{k} \qquad (10)$$

where

q/A = Heat flux across clad wall.
h = Clad wall thickness.
k = Clad thermal conductivity.

Usually $\epsilon_{\theta_{\Delta T_A}}$ values are relatively small ($\approx 3 \times 10^{-4}$) and therefore may be neglected in

comparison with $\epsilon_{\theta_{cl-u_A}}$. However, when the width of the plastic cycle loop is small

($\epsilon_B - \epsilon_D \approx 3 \times 10^{-3}$), the thermal strain should be included.

Then in terms of the strain state at operation, these are combined as

$$\epsilon_A = \epsilon_{\theta_{cl-u_A}} \pm \epsilon_{\theta_{\Delta T_A}} \qquad \begin{array}{l} + \text{ on coolant surface of clad} \\ - \text{ on fuel surface of clad} \end{array} \qquad (11)$$

Substituting (3) through (10). and rearranging, the clad strain at A is

$$\epsilon_A = \bar{\alpha}_f (\bar{T}_{f_A} - T_R) - \bar{\alpha}_{cl}(T_A - T_R) - \frac{\delta_{gap_R}}{\bar{D}} + \frac{\alpha_{cl_A}}{2} \frac{q}{A} \frac{h}{k} \qquad (12)$$

This strain may be used to determine an equivalent interference displacement which should be used in the strain reversal relations instead of the membrane displacement given by (7). This equivalent is

$$\delta int_A = \tilde{\delta} int_A + \bar{D} \epsilon_{\theta_{\Delta T_A}} = \bar{D} \epsilon_A \qquad (13)$$

These effects may be illustrated in the following diagram.

Note that strain in the cladding produced by the interference between fuel and clad is only that produced by the excess of fuel expansion over the sum of the clad expansion and the equivalent fabricated gap. Numbers within paranthesis refer to the appropriate equations. Note also that the strain increment, $\epsilon_A - \epsilon_{\tilde{A}}$, is that given by the thermal strain relation in (9).

3.3 Displacement Relations at Low Power

The simple cycle DABCD infers isothermal operation at T_A with the differential fuel expansions determined by the power levels P_A and P_C. However, for continuously cooled superheat reactors, the clad thermal inertia is small, and the power reduction is quickly followed by the clad temperature reduction to the lower power value T_C.

This can be accommodated by evaluating the displacements at a quasi-isothermal P_C condition. In a manner similar to that used to establish displacements at the high power condition, the lower power displacements can be determined. Thus, the fuel expansion referred to the fabrication temperature, i.e., room temperature, is

$$\delta_{fc} = \overline{D}\, \overline{\alpha}_{fc} \, (\overline{T}_{fc} - T_R) \tag{14}$$

where the expansion coefficient is now averaged over the range from T_R to T_C.

The relative clad displacement at the low power condition, P_C, is determined somewhat differently than at the P_A condition. The clad thermal expansion, referred to fabrication conditions at room temperature T_R, is

$$\delta_{cl_c} = \overline{D}\, \overline{\alpha}_{cl_c} \, (T_C - T_R) \tag{15}$$

where $\quad \alpha_{cl_c}$ Average expansion coefficient for range T_R to T_C.
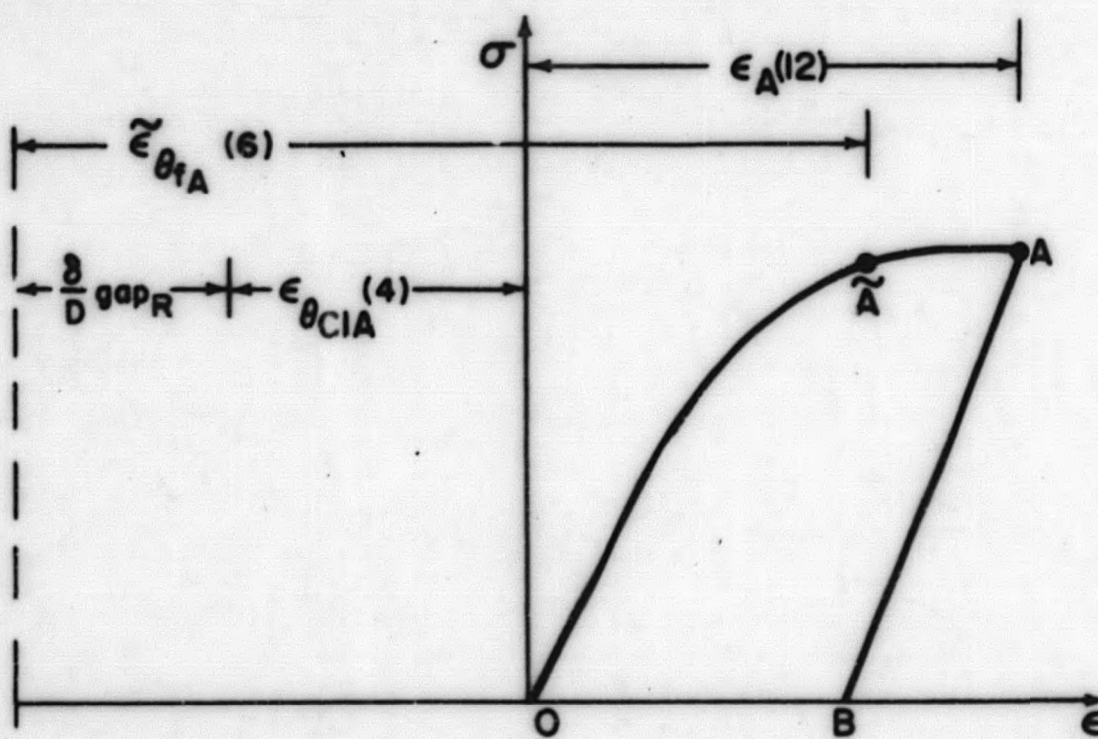
Figure 3.2. Clad Strain Diagram for Rated Power Condition

Also, on the outer surface of the clad there exists a permanent strain of magnitude ϵ_B, which was caused by the interference and thermal strain ϵ_A, and which was relieved by an amount equivalent to the elastic springback.

$$\epsilon_B = \epsilon_A - \frac{\sigma_A}{E} \tag{16}$$

The diametral gap at the low power condition can then be determined. This is the sum of the fabricated gap, the clad thermal expansion, and the equivalent permanent clad strain, less the fuel expansion.

$$\delta_{gap_c} = \delta_{gap_R} + \delta_{cl_c} + D\epsilon_B - \delta_{fc} \tag{17}$$

The relative magnitude of δ_{gap_c} will be used to establish which of the two forms the clad will assume at the low power condition.

Cladding Stability

At all times during operation the coolant pressure acts to produce compressive loads in the clad. (If fission product pressure cannot be considered negligible, the compressive loads would be produced by the difference between the coolant and fission product pressures. For this work, the fission product pressure will be assumed negligible.) For cladding geometries of interest, the clad may be unstable when subjected to the pressure loads, and so collapse against the fuel. A practical limit to the stability condition is that the cladding will collapse if $p > p_c$ where

$$p_c \approx \frac{0.15\,\overline{E}}{1 - \nu^2}\left(\frac{h}{\overline{R}}\right)^3 \tag{18}$$

where p = External coolant pressure

p_c = Critical collapse pressure

ν = Poisson's ratio at T_A

$\overline{R}$ = Mean radius of clad = $\overline{D}/2$

If $p < p_c$, the cladding will remain circular. Then the coolant pressure p will produce a membrane stress in the clad

$$\sigma_{\theta_p} = -p\frac{\overline{R}}{h} \tag{19}$$

where σ_{θ_p} = Membrane stress in the clad (hoop stress)

h = Clad thickness

. which will cause a circular contraction of the clad in accordance with the stress-strain curve of the clad. This is discussed later.

If $p \geq p_c$, the clad may not remain circular. The coolant pressure will cause the clad to change to either an elliptical or an oval shape if the gap $\delta_{gap_c} > 0$, which is usually always the case where cycling exists. These other geometries are shown below.

In addition to the membrane strain associated with the pressure hoop stress, the change to the non-circular shapes shown induce bending strains in the clad. An expression for the bending strain can be developed from the curvature change relations, and for the elliptical shape, may be written as

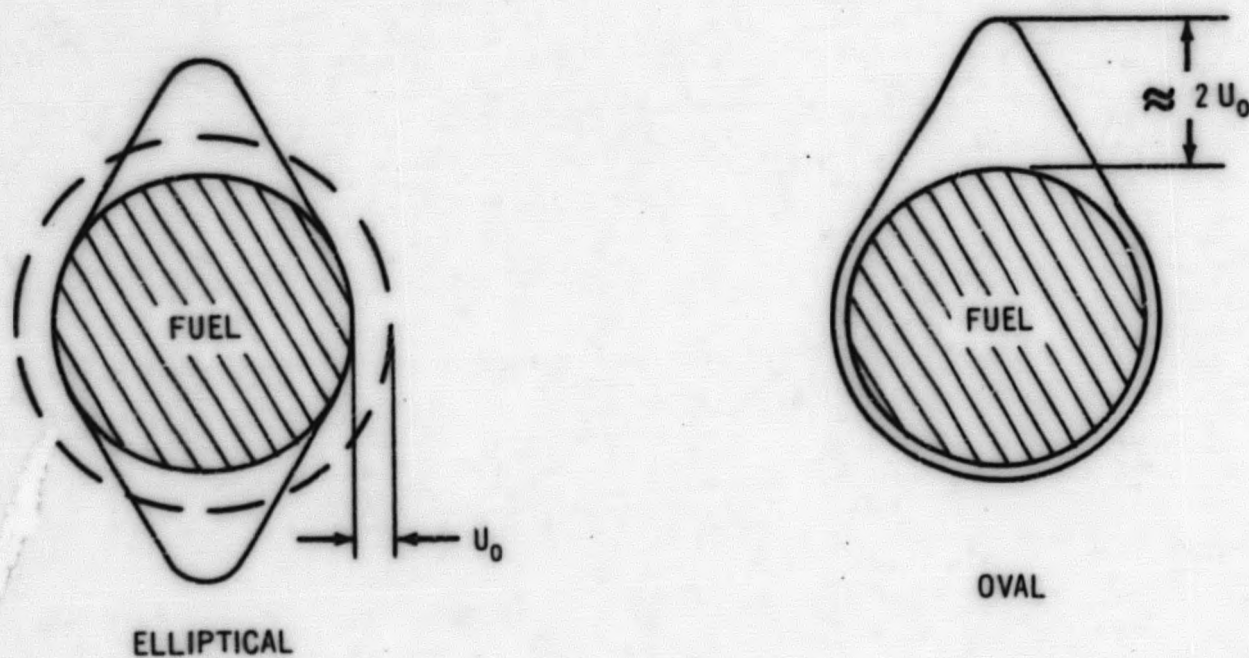$$\epsilon_{c_b} = -1.5 \frac{U_o h}{R^2} \tag{20}$$

where U_o = Uniform radial gap between fuel and clad at B

The radial gap is half the diametral gap, as from (17),

$$U_o = \frac{1}{2} \delta_{gap_c} \tag{21}$$

Substituting, the bending strain may be written as

$$\epsilon_{c_b} = -\frac{3}{4} \frac{\delta_{gap_c} h}{R^2} \tag{22}$$

ELLIPTICAL

OVAL

1216-3

Figure 3.3. Clad Geometries

where the minus sign is used since the maximum strain range is desired. The bending strain is superposed on the membrane strain to determine the largest negative or smallest positive strain level at P_c.

The bending strains associated with the oval shape are approximately twice those associated with the elliptical shape. However, the oval shape is also associated with the onset of wrinkle formation. This is discussed more fully in a later report, since the strain distribution involves two simultaneous changes of curvature at the peak and base of the wrinkle. So with negligible error for the uniform analysis, the bending strain will be considered that determined from (22). In general, the bending strain will be ≈ 5-10 percent of the membrane strain. At the lower strain level, ϵ_c, the compressive bending strain addition is most conservative, and occurs on the outer surface at the line of contact with the fuel.
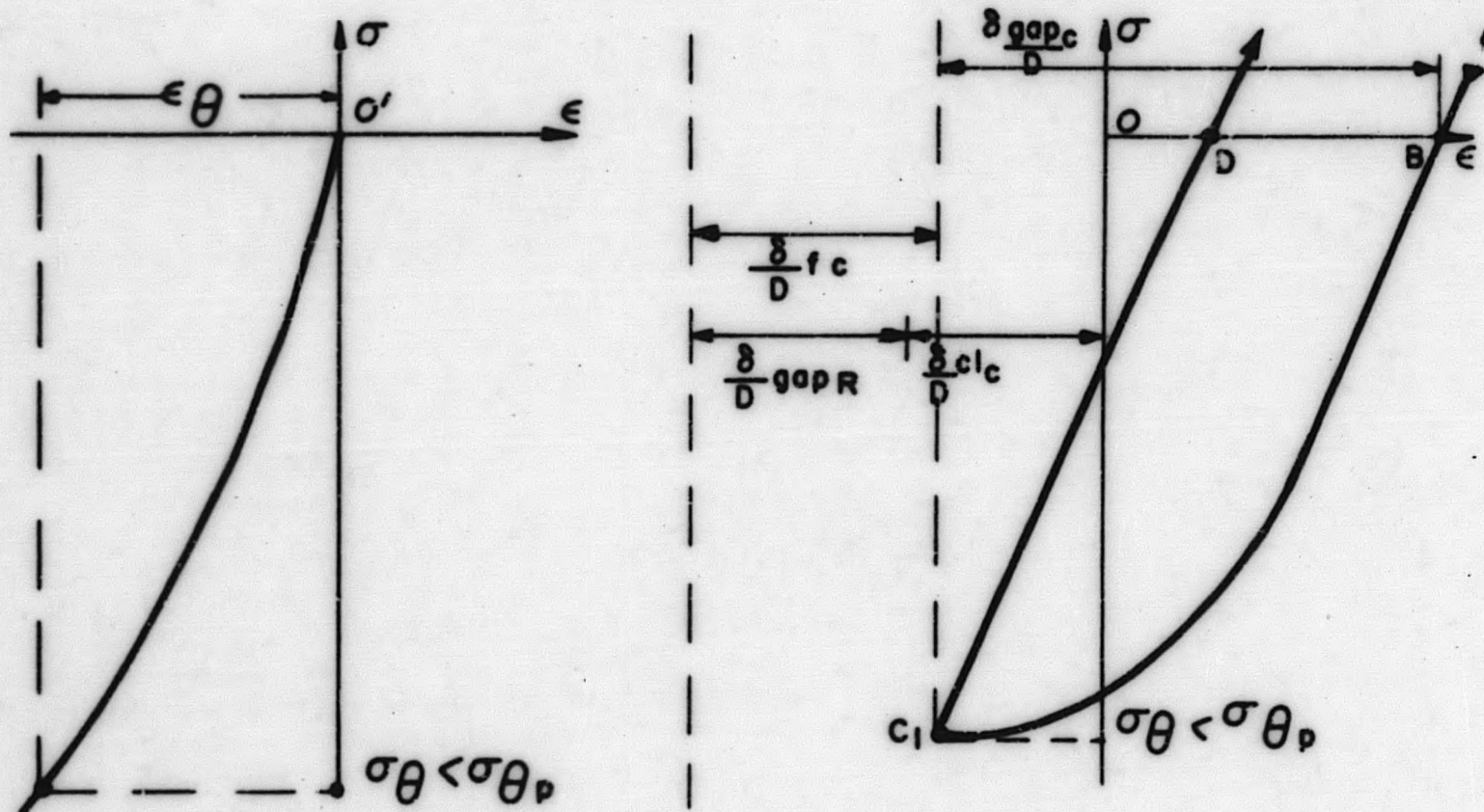
Gap Limiting

For some designs, the diametral gap, δ_{gap_c}, may be smaller than the diametral contraction of the cladding associated with the full development of the hoop stress, $\sigma_{\theta p}$ For those, the gap, and not the stress is the controlling factor. The contraction strain should be used to evaluate the clad stress σ_θ, which will always be less than $\sigma_{\theta p}$. Also, such a limitation will prevent the formation of any non-circular geometries, and so bending strains could not be developed.

Low Power Relations

The end points of the strain cycle condition, ϵ_c, may be discussed in terms of the following diagrams, with each case representing the effect of the gap δ_{gap_c} on the value of ϵ_c. The figures on the left are the compressive stress strain curves for the cladding, over the stress range $\sigma_\theta < \sigma_{\theta p}$ when the gap limits the clad deformation, and over the stress range $\sigma_{\theta p}$ when the gap is not limiting. The figures on the right represent the lower range of the power cycle. For case 1, the curve BC, is the stress-strain curve with the origin 0' located at B. For case 2, the curve BC_2 includes not only the associated stress-strain curve, but also the strain addition caused by bending. The other terms are those described previously. The thermal strains are not shown because at low power they are negligible.

3.4 Design Strain Relations

In a manner similar to that described by Coffin, the previously determined strain relations may be combined for design purposes. Consider the following diagram.

Case 1. Low Power Gap Limiting
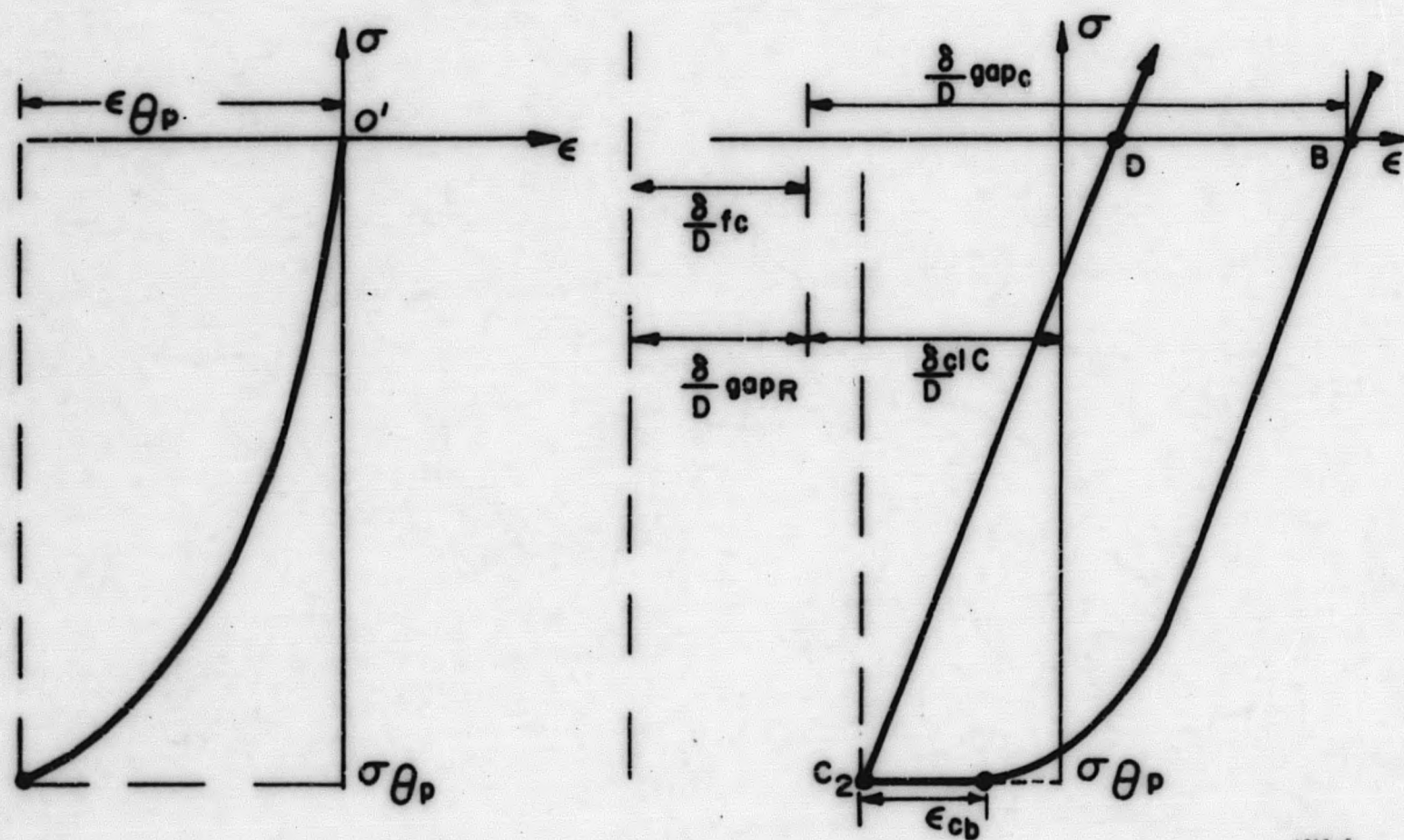
Case 2. Low Power Gap Not Limiting

Compressive Stress Strain

Lower Portion of Power Cycle

1216-6

Figure 3.4

NOTE:

C may be C_1 or C_2

$$\Delta \epsilon_e = \frac{\Delta \sigma}{E}$$

1216—5
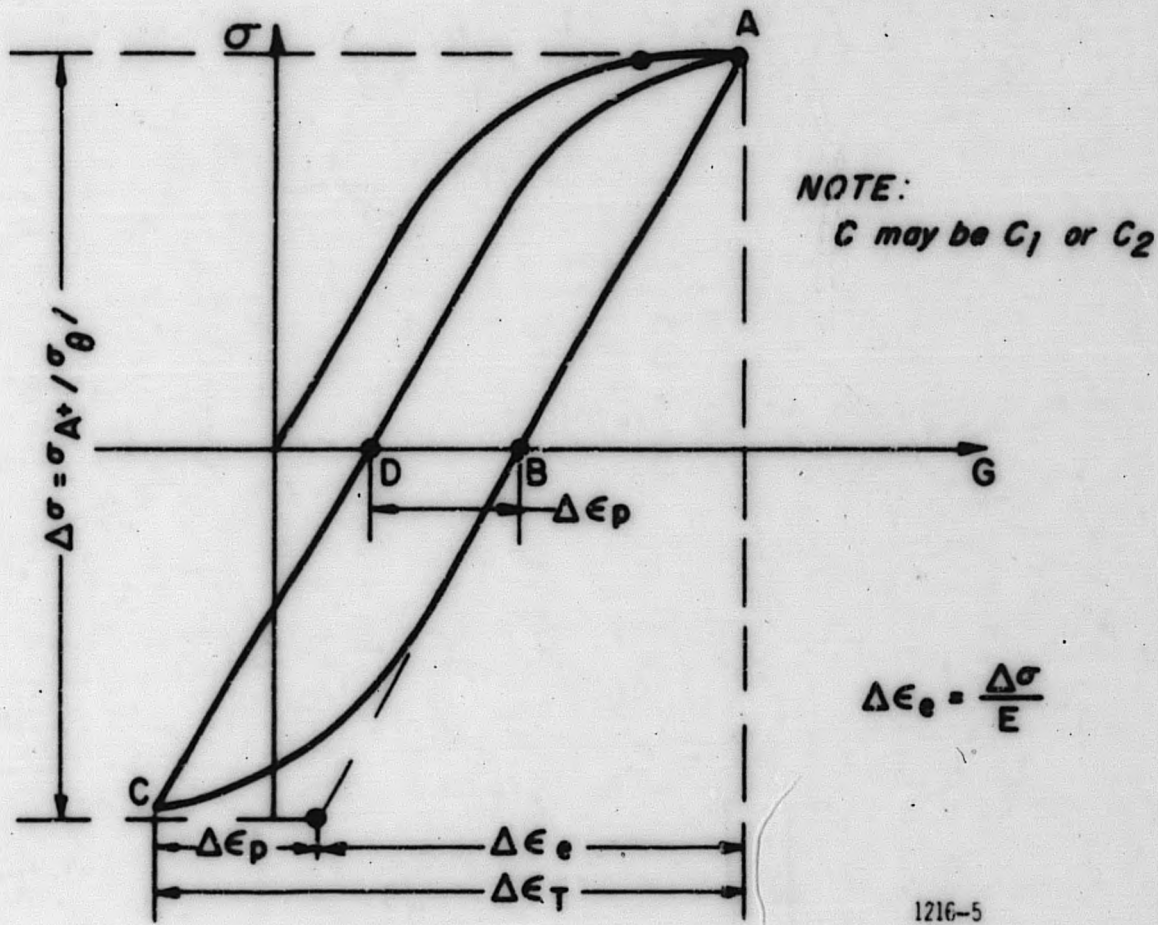
Figure 3.5.   Strain Power Cycle

The plastic portion of the cycle, $\Delta\epsilon_p = \epsilon_B - \epsilon_D$, may be determined from the difference between the total strain range $\Delta\epsilon_T$, and the elastic portion $\Delta\epsilon_e$.

$$\Delta\epsilon_p = \Delta\epsilon_T - \Delta\epsilon_e = \Delta\epsilon_T - \frac{\sigma_A + |\sigma_\theta|}{E} \tag{23}$$

$$\Delta\epsilon_T = \epsilon_A - \epsilon_c \tag{24}$$

Then the strain relations may be established for each of the design conditions.

Case 1 - When the gap limits fuel contraction $(\sigma_\theta < \sigma_{\theta p})$

$$\Delta\epsilon_{T_1} = \epsilon_A - \epsilon_{c_1} = \frac{\delta\, gap_c}{D} + \frac{\sigma_A}{E} \tag{25}$$

and

$$\Delta\epsilon_{p_1} = \frac{\delta\, gap_c}{D} - \frac{|\sigma_\theta|}{E} \qquad\qquad \text{(Also see equation (37))} \tag{26}$$

Case 2. When the gap does not limit fuel contraction ($\sigma_\theta = \sigma_{\theta p}$)

a. When the clad is unstable and bending is included. ($p \geq p_c$ of equation (18))

$$\Delta\epsilon_{T_{2_a}} = \epsilon_A - \epsilon_{c_2} = \frac{\sigma_A}{E} + \left| \epsilon_{\theta p} \right| + \left| \epsilon_{c_b} \right| \qquad (27a)$$

$$\Delta\epsilon_{p_{2_a}} = \left| \epsilon_{\theta p} \right| + \left| \epsilon_{c_b} \right| - \left| \frac{\sigma_{\theta p}}{E} \right| \qquad \text{(Also see equation (38))} \qquad (28a)$$

b. When the clad is stable and bending is neglected. ($p < p_c$ of equation (18))

$$\Delta\epsilon_{T_{2_b}} = \epsilon_A - \epsilon_{c_2} = \frac{\sigma_A}{E} + \left| \epsilon_{\theta p} \right| \qquad (27b)$$

$$\Delta\epsilon_{p_{2_b}} = \left| \epsilon_{\theta p} \right| - \left| \frac{\sigma_{\theta p}}{E} \right| \qquad \text{(Also see equation (39))} \qquad (28b)$$

The appropriate design strain relation, equations 26, 28a, or 28b, is substituted into equation 40 to determine the number of cycles to failure. However, each of these three relations is independent of creep effects. For superheat applications, the cladding is expected to perform at temperatures where creep may be significant, and where creep may cause an increase in the plastic strain range. A method by which such a displacement could be evaluated is described in the following section.

3.5 Uniform Cycling Creep Considerations

In terms of the displacement method, extended reactor operation at maximum power P_A would provide sufficient time for creep and relaxation changes to occur in the fuel cladding. With respect to the uniform cycling strain path, these can be lumped into a result that is a decrease of stress at constant strain ϵ_A. In effect, this means that some of the elastic strain is converted to time dependent permanent deformation strain. The equation

$$\epsilon_{A\ Total} = \epsilon_{A\ elastic} + \epsilon_{A\ plastic \atop load} + \epsilon_{A\ plastic \atop time} = constant \qquad (29)$$

defines the equivalence. As illustrated by the strain path, the plastic strain range without the time effect $\Delta\epsilon_p$, ($= \epsilon_B - \epsilon_D$), is increased to that including the time effect $\Delta\epsilon_{pt}$, ($= \epsilon_{Bt} - \epsilon_D$). The loop AA_tB_tCDA is produced, because during the interval at power, the stress σ_A is relaxed by an amount $\Delta\sigma_A$ to the value σ_{At}. Since the low power level conditions have not changed, (for the uniform cycling assumption), the end state point C remains approximately the same as before. (The shift of the compressive $\sigma - \epsilon$ curve may require a slight adjustment of ϵ_c to correspond to $\sigma_{\theta p}$).
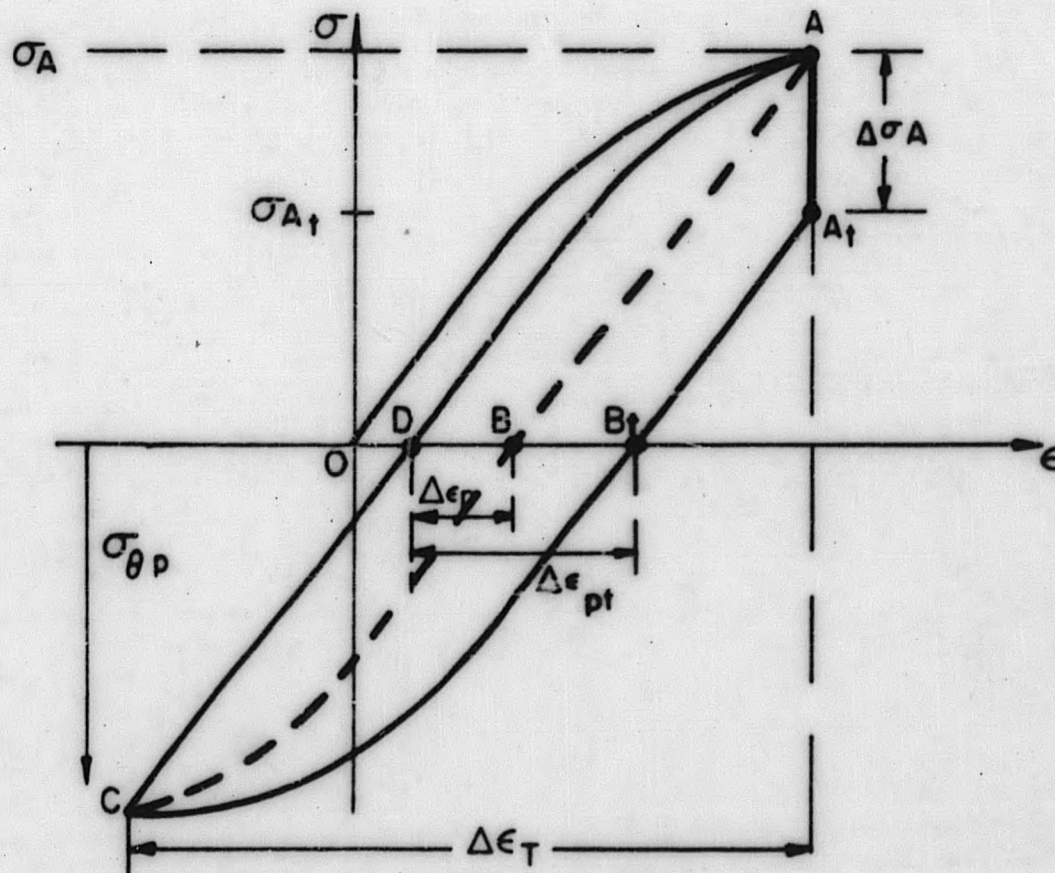
Figure 3.6.   Strain Path

1216-7

It will be emphasized again that this is a simplified consideration of uniform relaxation applied to a circular geometry, and non-uniform deformations are not considered at present. Subsequent reports will present superheat design techniques to account for non-uniform deformations such as those produced by either creep buckling, or plastic instabilities which lead to the formation of inelastic longitudinal wrinkles.   For additional information on these, the reader is referred to two papers; Poritsky[11] considers creep effects on cylindrical shell stresses, and Calladine[12] presents a finite difference technique by which the creep behavior of a wrinkle is described.

Here, the present concern is to describe a method by which the designer can evaluate $\Delta\sigma_A$ and the relative change to modify the $\Delta\epsilon_p$ used for failure calculations. The time involved in the change at ϵ_A of σ_A to σ_{A_t} is somewhat analogous to what Coffin defines as hold time[1]. In strain cycle experiments the time during which the specimen is held at the maximum strain level is considered to be the hold time.   Coffin has found that for specimens loaded to the same strain range, increased hold times are associated with decreased cycles to failure. Here, increased relaxation times cause increased plastic strain ranges, and so also should predict fewer cycles to failure.

-15-

If one assumes that during the relaxation from A to A_t, the plastic deformation caused by the fuel expansion does not change, then the relaxation or time dependent plastic strain change is developed at the expense of elastic strain. (This is associated with the shift of the unloading curve from B to B_t.) Thus

$$\epsilon_{el} + \epsilon_{pl-t} = 0 \tag{30}$$

and the time derivatives are also

$$\dot{\epsilon}_{el} + \dot{\epsilon}_{pl-t} = 0 \tag{31}$$

Since the elastic portion is considered in terms of only one dimensional stress and strain, using the elastic modulus to relate elastic stress and strain rates

$$\frac{\dot{\sigma}}{E} + \dot{\epsilon}_{pl-t} = 0 \tag{32}$$

For simplification, consider the constant creep rate law as

$$\dot{\epsilon}_{pl-t} = A\sigma^m \tag{33}$$

where   A, m = Material constants

For short times, this relation predicts too small a plastic strain change, but for times of interest to superheat, and considering the relatively high initial stress level, the simplification gained should over-ride the small degree of optimism of the final expression. Actually, considering the spread of most creep data, the use of the simple expression will not introduce too large an error. Then, substituting (33) and rearranging

$$\int_{\sigma_A}^{\sigma_{A_t}} \sigma^{-m} d\sigma = -EA \int_{t=0}^{t=t} dt \tag{34}$$

Solving, and rearranging, the final value of σ_{A_t} is given by,

$$\frac{1}{\sigma_{A_t}^{m-1}} = \frac{1}{\sigma_A^{m-1}} + (m-1) EAt \tag{35}$$

where   t = Hold time under consideration - (at power P_A)

Then the strain increment to be added to the plastic strain range is proportional to the stress change or

$$\epsilon_{B_t} - \epsilon_B = \frac{1}{E} (\sigma_A - \sigma_{A_t}) \tag{36}$$

The increment $\epsilon_{B_t} - \epsilon_B$ is then added to either $\Delta\epsilon_{p1}$ or $\Delta\epsilon_{p2}$ of equations (26 or 28) to obtain the plastic strain range $\Delta\epsilon_p$ used in the failure relation, (39). When this is done, the plastic strain range to be used for failure calculations is denoted by the bar, and is given by one of the following equations.

Case 1 - Gap Limiting

$$\Delta\bar{\epsilon}_{p_1} = \frac{\delta \, gap_c}{D} - \left|\frac{\sigma_{\theta}}{E}\right| + \frac{(\sigma A - \sigma A_t)}{E} \tag{37}$$

Case 2. Gap Not Limiting

a. Bending included

$$\Delta\bar{\epsilon}_{p_{2_a}} = \left|\epsilon_{\theta p}\right| + \left|\epsilon_{c_b}\right| - \left|\frac{\sigma_{\theta} p}{E}\right| + \frac{(\sigma A - \sigma A_t)}{E} \tag{38}$$

b. Bending not included

$$\Delta\bar{\epsilon}_{p_{2_b}} = \left|\epsilon_{\theta p}\right| - \left|\frac{\sigma_{\theta} p}{E}\right| + \frac{(\sigma A - \sigma A_t)}{E} \tag{39}$$

3.6 Displacement Cycles to Failure Relation

The recommended relation to predict the cycles to failure in terms of the plastic range is a modified Coffin-type expression. This is

$$N_f = k_f \left(\frac{c}{\Delta\epsilon_p}\right)^n \tag{40}$$

where N_f = Number of cycles to failure
$\Delta\epsilon_p$ = Plastic strain range (37, 38, or 39)
c, n = Material property constants
k_f = Reduction factor accounting for radiation, etc. (See Equation (46))

The uniform cycling failure relation (40) can be evaluated using the appropriate plastic strain range for the given design condition. As stated previously, the one-dimensional treatment of this section should be considered preliminary in nature since other factors, such as wrinkling are not included here. These will be presented in subsequent reports. However, that this simplified technique can be useful for preliminary evaluations has been indicated by experiment. Though other failure contributing conditions were present. (corrosion, etc.), the superheat SADE-4B experiment structural analysis predicted cyclic lifetimes that were 30 percent optimistic. i.e., actual cyclic lifetime was 70 percent of the predicted value.

3.7 Cumulative Life Cycles

Reactors do not always operate between the same power levels since the load requirements may vary. The suggested method of evaluating the accumulated fatigue damage is based in Miner's hypothesis. [13]

This is to evaluate N_f for each magnitude of power level change. If there are many different power level changes, the change ranges may be lumped into several groups, and an N_f determined from the average change for each group. Then one would obtain N_{f1}, N_{f2}, ----N_{fn} for each of the changes, or groups of changes. Letting n_1, n_2, ----n_n represent the expected number of cycles to be imposed, failure due to the mechanical cycling may be expected when

$$\frac{n_1}{N_{f1}} + \frac{n_2}{N_{f2}} + \cdots + \frac{n_n}{N_{fn}} = 1 \tag{41}$$

Attempted correlations of reactor data (not in the superheat range) indicate that the value 1 may vary by as much as 50 percent. This may reflect the presence of other conditions, such as corrosion. However, for purposes of estimating the cyclic performance of the cladding, use of the value 1 is recommended.

4. UNIFORM STRAIN CYCLING - STRESS METHOD

An alternate method to predict low cycle fatigue is suggested for use in design. This method is based on stress values rather than displacements as above. Experimental verification of the alternate method is in progress, and the results will be presented in subsequent reports.

4.1 Stress Cycle Relation

Tavernelli and Coffin[4] have reported experimental confirmation of a low cycle fatigue relation proposed by Langer[5] to the ASME Boiler and Pressure Vessel Committee.

The relation is

$$S = \frac{Ec}{2N^{1/2}} + S_e \qquad \text{(Author's equation 3)} \qquad (42)$$

where

S = Elastically computed stress amplitude

E = Young's modulus of elasticity

c = Materials property constant derived from reduction of area data

N = Cycles to failure

S_e = Endurance limit

which may be written as

$$N = \frac{1}{4} \left[\frac{Ec}{S - S_e} \right]^2 \qquad \text{(See also equation (46))} \qquad (43)$$

As stated by the authors, (42) has the advantage of being very practical for design purposes, since S could be compared directly with elastic stress values determined by standard stress analysis techniques.

The paper[4] illustrated good correlation between experiment and theory for various materials, including 347 stainless steel and nickel A. This is to be expected since the stress relation was established by adjustment of the strain relation $N_f \Delta\epsilon_p^n = C$. Though the tests were conducted at room temperature, the results indicated that it would be reasonable to extrapolate the technique to higher temperature conditions typical of superheat operation.

4.2 Relation Parameter Values

The values of the parameters used in the relation (42) are readily available in the literature for many materials of interest, but primarily for room temperature conditions. At temperatures of interest for superheat applications (800-1400 F), reliable modulus of elasticity values are usually available, but endurance limit values may not be. Accurate values of the endurance limit S_e at the design temperatures should be used if available. However, if S_e is not available, a reasonable, but slightly optimistic cyclic life value may be obtained by using the 0.2 percent offset yield strength.

As shown in reference 4, the parameter C may be determined from reduction in area values determined in tensile tests. This would be

$$C = -\frac{1}{2} \ln \frac{100 - \% RA}{100} \qquad \text{(Author's equation 2)} \qquad (44)$$

where

$$\% RA = \frac{Ao - A}{Ao} \times 100$$

Ao = Initial area of tensile test specimen

A = Final area of tensile test specimen

4.3 Design Application of Stress Cycle Relation

Relation (42) was shown by Tavernelli and Coffin to accurately predict the experimental data available from the strain cycling tests listed in their paper.[4] In general, these data were obtained from uniaxial tests which did not involve biaxial stresses.

However, the relation was developed for use by pressure vessel designers, and pressure vessels are subjected to multiaxial stresses. In line with pressure vessel design techniques, where the maximum stress is calculated, and the calculated value is compared with an allowable stress value for specified operating conditions (i.e. material temperature), it is assumed the technique can be established whereby the S value can be considered equivalent to the maximum elastic stress amplitude of either of the two biaxial stresses.

Some additional work is required to establish this. An evaluation of the SADE-4B experiment by the stress method predicted a cyclic lifetime more than an order of magnitude greater than that measured. (It is recognized that other lifetime reducing mechanisms were present in the SADE-4B experiment, such as the corrosive environment. However, on a structural basis only, the displacement method predicted results only 30 percent in error).

At present, it appears that if confirmed by experiment, the stress method would be preferable to the displacement method for application to superheat design. It is more amenable to analysis, and would not require the sometimes difficult to obtain extended strain range material property curves. A more comprehensive evaluation of this method will be presented in a subsequent report. At present, the only other evaluation in this report is based on $S = \Delta\epsilon_T \cdot E$ with the $\Delta\epsilon_T$ values compared to the other data in section 5. Note that the authors define the stress amplitude in terms of the total strain range $\Delta\epsilon_T$ by the relation

$$S = \frac{\Delta\epsilon_T \cdot E}{2} \qquad (45)$$

The two forms of S are compared in the following section.

5. COMPARISON OF EXPERIMENTAL DATA

One of the objects of the strain cycling task of the superheat program was to establish the effect, if any, of fast neutron flux on the strain cycling performance of cladding for superheat applications. This has been completed, in part, by Reynolds; some results have been presented in his interim report. [6] As he states, "One of the most significant results of the testing program was the determination of the three-fold reduction of cyclic lifetime because of radiation". Work is continuing, but this available result should be used in all superheat fatigue design calculations. As applied in this report, the coefficient k_f of equation (40) should be 0.33. Then (41) may be revised to a form accounting for radiation damage as

$$N_{f_{rad}} = 0.33 \left(\frac{c}{\Delta\epsilon_p} \right)^n \tag{46}$$

(Note also that the radiation damage effect can be factored into the stress cycle relation by changing the value of the coefficient from 1/4 to 1/12.)

Another object was to evaluate the results of the experimental work, and to develop analytical techniques to utilize the results in the design of fuel cladding for superheat reactor applications.

5.1 Experimental Data from this Program

As may be seen from Reynolds' report, several materials have been evaluated at temperatures of interest to superheat applications. These data were obtained for the cycling frequency of two per hour. The number of cycles to failure without radiation was shown as a function of both total and plastic strain ranges. Then, in terms of the equation

$$N_{f_{no-rad}} = \left(\frac{c}{\Delta\epsilon_p} \right)^n \tag{47}$$

these data may be tabulated as follows in Table 5.1, and are illustrated in Figure 5.1

Table 5.1

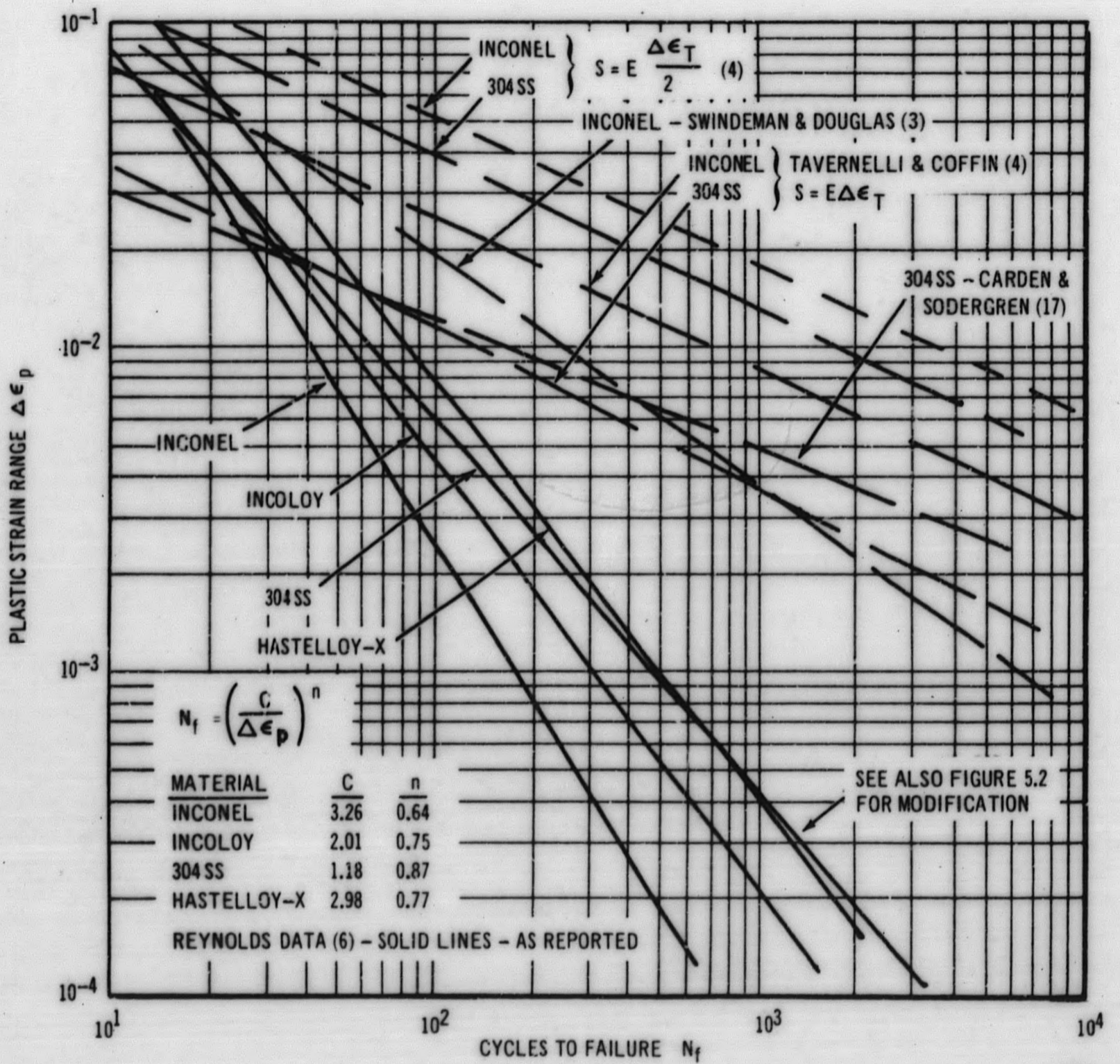| Material	Temperature	C	n
304 SS	1300 F	1.18	0.87
Inconel	1300 F	3.26	0.64
Incoloy	1300 F	2.01	0.75
Hastelloy-X	1300 F	2.98	0.77

Figure 5.1.   Plastic Strain Range vs Cycles to Failure at 1300 F
Without Radiation Effects

Several data points were also presented which illustrated the radiation damage effect. Before these data are applied by the recommended equations, some comparison with data in the literature should be made, and also the recommended equations should be applied to those superheat designs which have already been tested, for comparison of predicted and actual performance. The latter has already been discussed.

5. 2 Consideration of the Radiation Effect Determined from this Program

The three-fold reduction of the number of cycles to failure of the cladding, when exposed to fast neutron irradiation, is significant to the cladding design, and should be factored into the design.

However, the factor of three was determined experimentally. While this is useful as a design criteria, and indeed is recommended as such, an analytic relation is desired which could be applied to a range of materials over a range of temperatures. One such relation investigated is Coffin's material parameter c, which is related to the fracture ductility and the reduction of area, (equation 44). Some data have been presented in the literature which illustrate the effect of irradiation on the reduction of area values for several materials. [14, 15, 16] Unfortunately, none of these apply directly to the materials and conditions of Reynolds' experiments. However, when the stainless steel and Inconel X data are evaluated, some interesting results are obtained.

A cyclic lifetime radiation effect in the range of 0. 2 to 0. 5 can be obtained in the following manner. From the reduction of area data for the irradiated and unirradiated material, determine the c parameter for each condition. The square of the ratio of the c for irradiated material to the c for the unirradiated material usually is in the range of 0. 2 to 0. 5. (The square is chosen because Coffin has found the wide range of applicability of that exponent to describe the cyclic lifetime of many ductile materials). The value so determined is a factor that can be used to multiply the unirradiated cyclic lifetime so as to estimate the irradiated cyclic lifetime.

The same procedure should also be applicable for estimating the difference of cyclic lifetimes between initially annealed and hardened materials.

The range 0. 2 to 0. 5 includes the 0. 33 value determined experimentally. This approach appears promising, and additional work will be presented in subsequent reports. For the present, the 0. 33 reduction factor is the value recommended for superheat fuel clad design.

5. 3 Experimental Data from the Literature

Two of the several strain cycling data sources in the literature will be compared with Reynolds' data. These are the papers by Swindeman and Douglas[3] and by Carden and Sodergren[17]. These were chosen primarily because test data was obtained at 1300 F on Inconel[3] and 304 SS[17]; these data may be compared directly without adjustment for temperature. Examination of Figure 5. 1 indicates that the 304 data obtained at the University of Alabama[17] has a flatter

slope than that of Reynolds', with a crossover at 40 cycles, and for lower strain ranges, predicts cyclic lifetimes considerably greater than do those of Reynolds. Similarly, the Inconel data from ORNL[3] predicts much longer cyclic lifetimes for all values greater than 10 cycles.

Two additional curves are shown for 304 SS and Inconel which were calculated according to the stress relation described by Tavernelli and Coffin[4], and listed here as equation (43). All parameters were evaluated for material properties at 1300 F, and the stress amplitude S was established from the total strain range reported by Reynolds with the modulus of elasticity at 1300 F. In equation form

$$S = E \, \Delta \epsilon_T \tag{48}$$

As defined by the authors, the stress amplitude S is equal to one half the product of the modulus and the total strain range. Both the authors' values S, and that given by equation (48) are shown in Figure 5.1. It can be seen that the (48) relation is a better fit to the literature data.

In general, the stress amplitude relation predicts cyclic lifetimes in approximately the same manner as the ORNL and University of Alabama data. This is not very surprising since the stress amplitude was correlated with, and substantiated by, strain cycling data previously obtained by Coffin and others, which is similar to that of ORNL and University of Alabama.

5.4 Comparison of Experimental Data

The question arises as to reasons why the various data differ so markedly for plastic strain levels of 1 percent and below, the experimental technique always being the first suspect. In contrast to the tests reported[3, 4, 17], laboratory type specimens were not used. Practical requirements dictated that commercial reactor grade tubing be used for the specimens. This almost automatically loosened the geometrical tolerances, in the form of eccentric tubing of varying wall thickness. An attempt was made to limit the effect of the variations by adjusting the mandrel dimensions slightly to accommodate the individual specimens, but even this could not alleviate all of the geometrical variations.

Another possible reason may be based on the stability of the specimen when subjected to external pressure on the outer surfaces. It can be shown by elastic stability methods[18] that the actuating pressures could cause an instability that would result in the formation of a number of longitudinal wrinkles similar to those illustrated in Figure 12 of reference 6. For the geometries and pressure ranges used, these lobes were calculated to range in number from seven to twelve. These lobes, though determined by elastic calculations, should locate positions where plastic hinges may be expected to develop.

Based on the assumption that twelve lobes were formed equidistant around the circumference, an estimate was made of the possible increases of reversed plastic strain because of extension and bending to those extensional membrane strains established by the mandrel geometry. The lobes were considered sinusoidal perturbations to the mean radius of the specimen.

The additional extensional strain was evaluated by use of elliptic integrals and was found to be negligible. However, the inextensional bending was calculated to produce significant strain additions. Based on the sinusoid, the perturbation curvature was calculated to be

$$\Delta \text{ Curvature} = \frac{n^2}{2R_m} \Delta \epsilon_T = \Delta K \tag{49}$$

where n = Number of lobes ($n = 12$)

R_m = Mean radius of specimen

$\Delta \epsilon_T$ = Total strain range reported

From this the perturbation bending strain was determined from

$$\Delta \epsilon_b = \frac{h}{2} \Delta K = 0.92 \Delta \epsilon_T \tag{50}$$

where

h = Specimen wall thickness (0.016-inch)

Then for any value of reported plastic strain $\Delta \epsilon_{pr}$, the modified result can be written as

$$\Delta \epsilon_{pm} = 1.92 \Delta \epsilon_{pr} + 0.0018 \tag{51}$$

where the 0.0018 is the approximate correction to account for the elastic strain.

Using (51), the reported data shown in Figure 5.1 were modified and illustrated in Figure 5.2. The saddle shape of the modified curves was caused by the somewhat arbitrary application of the sinusoid, regardless of strain amplitude, and also by the interpretation of the reported $\Delta \epsilon_T$ curves as they were modified by the bending strain (50).

A review of Figure 5.2 indicates that the data, in modified form as compared to the form reported, are better fit with data from other sources, though the curve shape is not. However, because most of the literature data were obtained from tests on laboratory type specimens, and the super-heat data were obtained from commercial tubing specimens, possible factors not evaluated at present may cause the differences shown by Figure 5.1
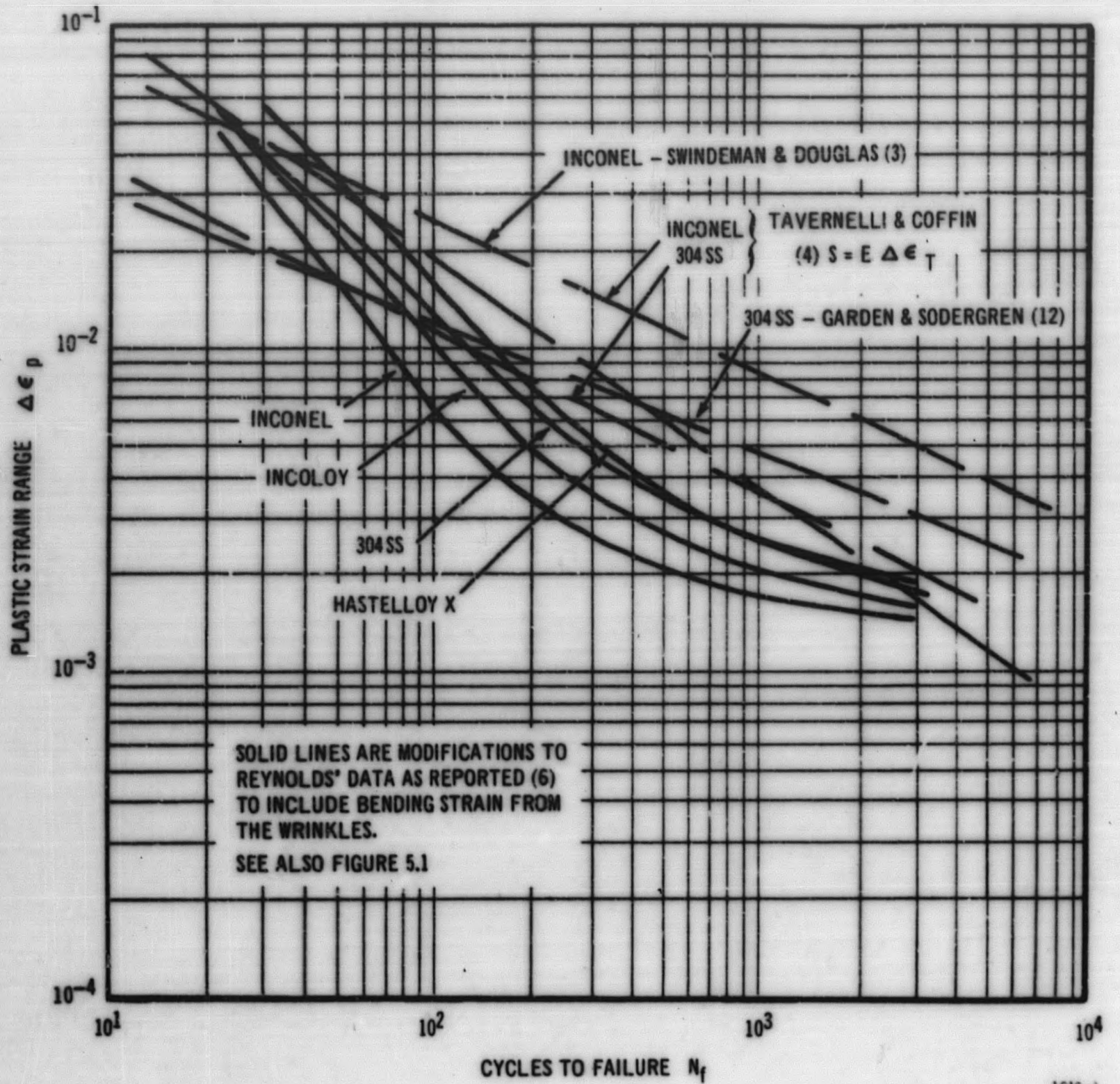
Figure 5.2. Plastic Strain Range vs Cycles to Failure at 1300 F without Radiation Effects Reported and Modified Values

An additional series of tests on thicker wall specimens (0.028 inch) are being performed at present in an attempt to establish whether or not stability effects provide distortions to the reversed plastic cycling range, and also some quantitative measure of the distortion, if so determined.

For the present, the probably extremely conservative recommendation is made that for application to superheat designs, the cyclic performance curves reported by Reynolds and illustrated in Figure 5.1, be used. Additional experimental and analytical work will probably indicate that this recommendation will be changed in the future, but for the present, the conservative approach is suggested.

6. CONCLUSIONS

The conclusions obtained from the work presented in this report, and the references, are:

1. Two simplified methods are available to define, for the designer, the predicted cyclic lifetime of superheat cladding. These are:

    a. Displacement method - Equation (46), where the material constants are presented in Table 5.1, and the plastic strain range is given by equations 37, 38, or 39.

    b. Stress method - Equation (43) with coefficient 1/4 replaced by 1/12 to account for radiation damage

2. Based on the SADE-4B performance evaluation, the cyclic data reported by Reynolds[6], and shown in Figure 5.1, are the presently recommended lifetime data to be used for superheat design.

3. A more comprehensive analytical method which accounts for biaxial and local effects as well as the uniform cycle is required; this will be presented in a subsequent report. However, the uniform cycle evaluation is adequate for preliminary design.

4. Other potential performance limitations, such as corrosion, are not considered in this evaluation, but they should be factored into the over-all design.

NOMENCLATURE

A, C, n, m   = Material property constants.

A, Ao   = Area, as used in equation 44.

$\bar{D}$ = Mean diameter of the cladding.

E   = Young's modulus of elasticity.

h   = Wall thickness

k   = Thermal conductivity.

k_f = Cycles to failure radiation reduction factor.

N_f = Number of cycles to failure.

p   = Pressure.

P   = Reactor or fuel power.

q/A   = Thermal heat flux.

R   = Mean radius of cladding.

S   = Elastic stress amplitude of the power cycle.

t   = Time

T   = Temperature

U_o = Radial gap between fuel and clad.

α = Thermal coefficient of expansion.

δ = Diametral displacement.

$\epsilon, \epsilon_\theta$ = Unit strain, unit strain in circumferential direction.

σ = Stress.

$\dot{\sigma}, \dot{\epsilon}$ = Time derivatives of stress, strain.

ν = Poisson's ratio.

Subscripts:

cl   = Clad.

cl-u   = Interference between clad and fuel, not including thermal gradient strain.

f   = Fuel.

gap   = Gap existing between fuel and clad

int   = Interference between clad and fuel, including thermal gradient strain.

p   = Plastic strain range. or pressure induced membrane stress.

T   = Total strain range.

ΔT = Thermal gradient induced strain.

A, B, C, D   = State points on path of power cycle.

REFERENCES

1. Coffin, Jr. L. F. "A Study of the Effects of Cyclic Thermal Stresses on a Ductile Metal," Transactions ASME, August 1954.

2. Manson, S. S. "Behavior of Materials Under Conditions of Thermal Stress", Heat Transfer Symposia, University of Michigan Engineering Research Institute, 1953.

3. Swindeman, R. W. and Douglas, D. A. "The Failure of Structural Metals Subjected to Strain Cycling Conditions", Transactions ASME 81D, p. 203, June, 1959.

4. Tavernelli, J. F. and Coffin, Jr., L. F. "Experimental Support for Generalized Equation Predicting Low Cycle Fatigue", Transactions ASME 84D, p. 533, December, 1962.

5. Langer, B. F. "Design of Pressure Vessels for Low Cycle Fatigue", Transactions ASME 84D, p. 389, September, 1962.

6. Reynolds, M. B. "Slow Cycle Strain Fatigue in Thin Wall Tubing", Preliminary Report, GEAP-3983, General Electric Company, AEC Informal Research and Development Report, July, 1962.

7. Beile, J. Editor, "Uranium Dioxide: Properties and Nuclear Applications", Naval Reactors Handbook, USAEC, 1961.

8. Hankel, R. ,"Stress and Temperature Distributions", NUCLEONICS, 18, 11, November, 1960.

9. Lyons, M. F. , Comprelli, F. A. , Hazel, V. E. and Townsend, H. E. , "Plastic Strain in Thin Fuel Element Cladding Due to UO_2 Thermal Expansion", GEAP-3739, General Electric Company, AEC Informal Research and Development Report, July 7, 1961.

10. Den Hartog, J. P. ,"Advanced Strength of Materials", McGraw Hill, 1952, p. 238.

11. Poritsky, H. , "Effect of Creep on Stresses in Cylindrical Shells", Creep in Structures Colloquium, Stanford University, July 1960, Editor, N. J. Hoff, Academic Press, 1962.

12. Calladine, C. R. "On the Creep of a Wrinkle", Creep in Structures Colloquium, Stanford University, July 1960, Editor, N. J. Hoff, Academic Press, 1962.

13. Miner, M. A. , "Cumulative Damage in Fatigue", Transactions ASME 67, p. 159, 1945.

14. Reactor Materials Quarterly, Vol 5, No. 3, USAEC, August, 1962, p. 53.

15. Joseph, J. W. , "Stress Relaxation in Stainless Steel During Irradiation", DP-369, E. I. du Pont de Nemours and Co. , USAEC Research and Development Report, June, 1959.

16. Schreiber, R. E. , "Mechanical Properties of Irradiated Stainless Steels", DP-579, E. I. du Pont de Nemours and Co. , USAEC Research and Development Report, September, 1961.

17. Carden, A. E. and Sodergren, J. H. , "The Failure of 304 Stainless Steel by Thermal Strain Cycling at Elevated Temperature", ASME Paper 61-WA-200, August, 1961.

18. Timoshenko, S. P. and Gere, J. M. , "Theory of Elastic Stability", 2nd Edition, McGraw Hill, 1961, Chap. 11.

END